MacroH2A Allows ATP-Dependent Chromatin Remodeling by SWI/SNF and ACF Complexes but Specifically Reduces Recruitment of SWI/SNF[†]

Evelyn Y. Chang,[‡] Helder Ferreira,[‖,§] Joanna Somers,[‖] Dmitri A. Nusinow,[‡,⊥] Tom Owen-Hughes,*[,‖] and Geeta J. Narlikar*[,‡]

Department of Biochemistry and Biophysics, University of California, San Francisco, California 94158, and Wellcome Trust Centre for Gene Regulation and Expression, College of Life Sciences, University of Dundee, Dundee DD1 5EH, Scotland

ABSTRACT: The variant histone macroH2A helps maintain X inactivation and gene silencing. Previous work implied that nucleosomes containing macroH2A cannot be remodeled by ISWI and SWI/SNF chromatin remodeling enzymes. Using approaches that prevent misassembly of macroH2A nucleosomes, we find that macroH2A nucleosomes are excellent substrates for both enzyme families. Interestingly, SWI/SNF, which is involved in gene activation, preferentially binds H2A nucleosomes over macroH2A nucleosomes, but ACF, an ISWI complex implicated in gene repression, shows no preference. Thus, macroH2A may help regulate the balance between activating and repressive remodeling complexes.

Incorporation of variant histones into nucleosomes is one major method by which cells regulate the function of specific chromatin regions. One example is found on the inactive X chromosome in female mammals, which is enriched in the H2A variant macroH2A. MacroH2A consists of three regions: an N-terminal histone domain, a 38-residue linker region, and a C-terminal macro domain that, at 25 kDa, is almost twice the size of H2A (*1*). Incorporation of macroH2A into the inactive X is thought to play an important role in maintaining silencing through subsequent cell divisions (*2, 3*). MacroH2A is also important for constitutive silencing of some autosomal genes, such as the IL-8 gene in B cells, and is enriched in senescence-associated heterochromatic foci, domains of repressed transcription associated with cell aging (*4, 5*).

The mechanism by which macroH2A contributes to gene silencing remains unknown. Recent biochemical experiments have suggested that nucleosomes containing the macro domain completely fail to be remodeled by both yeast SWI/SNF and *Drosophila* ACF, members of the SWI/SNF and ISWI families of ATP-dependent chromatin remodeling complexes, respectively (*6, 7*). Further, these studies implied that nucleosomes containing just the histone domain of macroH2A cannot be remodeled by yeast SWI/SNF (*7*). These results were surprising on two fronts. First, while SWI/SNF complexes are generally involved in transcriptional

activation, ACF complexes are almost exclusively involved in transcriptional silencing. Thus, it was unexpected that macroH2A nucleosomes would be poor substrates for ACF. Second, subsequent crystal structures of nucleosomes containing the histone domain of macroH2A show it to be structurally very similar to H2A nucleosomes (*8*). Thus, it was not clear how the histone domain alone could interfere with nucleosome remodeling.

These unexpected results may partly be explained by the recent observation that macroH2A is more likely than H2A to form noncanonical nucleosome structures when assembled in vitro. In these studies nucleosomes assembled from histone octamers were found to be composed of two species, one of which is refractory to heat shifting and hypothesized to contain a noncanonical histone composition (*9*). Our two laboratories independently addressed this possibility using macroH2A nucleosomes assembled with controls against noncanonical nucleosome structures. We find that, contrary to previous results, our macroH2A nucleosomes are good substrates for activity with both SWI/SNF and ACF complexes. We further show that, under direct competition conditions. SWI/SNF complexes preferentially bind H2A nucleosomes over macroH2A nucleosomes, while ACF shows no preference.

EXPERIMENTAL PROCEDURES

Protein Purification. The FLAG-tagged hSWI/SNF complex was affinity purified as described previously from HeLa nuclear extracts obtained from the National Cell Culture Center (*10*). TAP-tagged RSC and ySWI/SNF were affinity purified from *Saccharomyces cerevisiae* as described previously (*11*). The human ACF complex was assembled and purified from Sf9 cells as previously described (*12*).

Nucleosome Assembly. Nucleosomes used for chromatin remodeling by the human enzymes were based on a DNA template containing the 601 positioning sequence, modified as previously described to contain a *Pst*I restriction site 18

* To whom correspondence should be addressed. E-mail: t.a.owenhughes@dundee.ac.uk or gnarlikar@biochem.ucsf.edu.
‡ University of California.
§ Current address: Friedrich Miescher Institute, Basel, Switzerland.
‖ University of Dundee.
⊥ Current address: Department of Cell and Developmental Biology, University of California at San Diego, La Jolla, CA 92093.
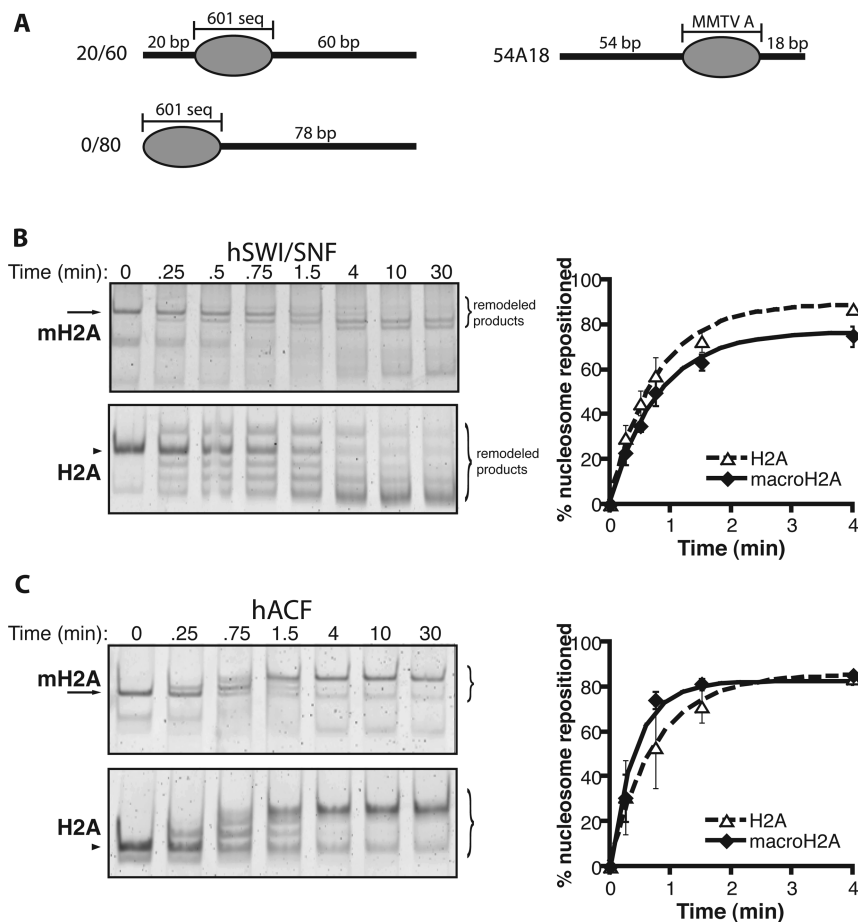
FIGURE 1: MacroH2A is a good substrate for ATP-dependent remodeling. (A) DNA constructs used to assemble nucleosomes. 20/60 and 0/80 nucleosomes are positioned using the 601 sequence. 54A18 nucleosomes are positioned on the MMTVA sequence. Numbers represent the length of flanking DNA on each side. (B) Native gel shift showing remodeling of 20/60 H2A and macroH2A (mH2A) nucleosomes by hSWI/SNF (left). $k_{obs} = 1.3 \pm 0.11$ min^{-1} for H2A nucleosomes and 1.3 ± 0.080 min^{-1} for macroH2A nucleosomes (right). (C) Native gel shift showing remodeling of 0/80 nucleosomes by ACF (left). $k_{obs} = 1.3 \pm 0.15$ min^{-1} for H2A nucleosomes and 2.4 ± 0.50 min^{-1} for macroH2A nucleosomes (right). Values are calculated from three independent experiments; error bars show the standard deviation. Long arrows mark unremodeled macroH2A nucleosomes; arrowheads mark unremodeled H2A nucleosomes.

bp from one end (*13*). DNA constructs were generated by PCR using primers complementary to various sites flanking the 601 sequence (sequences available upon request). Two templates were generated. One contained the 601 site at one end and 78 bp of flanking DNA on the other (0/80 template). The other template contained 20 and 60 bp of flanking DNA on either side of the 601 sequence (20/60 template). 0/80 DNA was used for assembly of nucleosomes for hACF assays, whereas the 20/60 DNA template was used for assembly of nucleosomes for hSWI/SNF assays. For the experiments depicted in Figure 4, H2A nucleosomes contained DNA end-labeled with Cy3 and mH2A-HD[1] nucleosomes contained DNA end-labeled with Cy5. These fluorescent labels were incorporated by using appropriately end-labeled fluorescent primers.

Nucleosomes used for chromatin remodeling by the yeast enzymes were based on the MMTV nucleosome A sequence. DNA was generated by preparative PCR using fluorescently labeled primers from Eurogentec. The PCR-amplified DNA fragments were purified by ion exchange chromatography on a 1.8 mL SOURCE 15Q (Pharmacia) column. The DNA fragments used were amplified from the MMTV nucleosome

A sequence. We have adopted the nomenclature of 54A18, to describe a 54 bp extension upstream and 18 bp extension downstream. The oligos used to generate fragment 54A18 were 5′TATGTAAATGCTT ATGTAAACCA and 5′TACA-TCTAGAAAAAG GAGC. For the experiments depicted in Figure 3b, the DNA used to assemble H2A nucleosomes was end-labeled with Cy3 and that used for mH2A nucleosomes with Cy5.

MacroH2A1.2 was expressed and purified as a dimer with H2B from BL21(DE3)-pLysS cells (Stratagene). A pCDF-Duet-1 plasmid encoding both H2B and a C-terminal two-Flag-tagged macroH2A1.2 was transformed into BL21(DE3)-pLysS cells and used to seed 50 mL starter cultures grown overnight to saturation with selection in both chloroamphenicol and spectinomycin. Starter cultures were used to seed 2 L of antibiotic-selected medium and grown to approximate absorbances of 0.7–0.8 before induction with 0.4 mM IPTG for 3 h. MacroH2A/H2B dimer was then purified first through a FLAG affinity column and subsequently diluted to 0.1 M NaCl. Nucleotide and DNA contaminants were removed by incubation with Q resin in batch for 30 min. The supernatant was removed and bound in batch to SP resin for 1 h. Bound resin was loaded onto a column and washed with 10–20 column values (c.v.) of

---

[1] Abbreviations: mH2A, macroH2A; macroH2A-HD, histone domain of macroH2A.
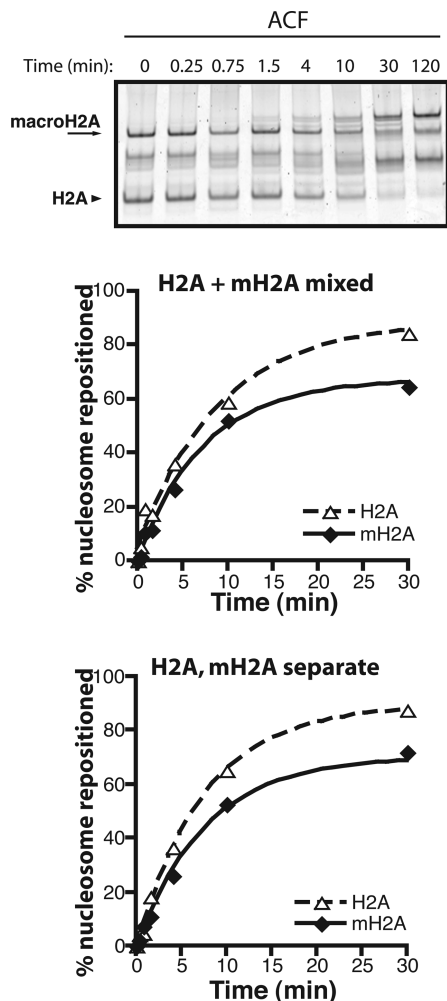
FIGURE 2: ACF is recruited equally well to H2A and macroH2A nucleosomes. In the top panel, 80 nM H2A and 80 nM macroH2A 0/80 nucleosomes were mixed with 5 nM hACF and visualized on the same gel. The larger macroH2A nucleosomes run much more slowly than H2A nucleosomes. In the middle panel, initial rates from the top panel are 10.5 ± 0.90 nM min^{-1} for H2A and 7.5 ± 0.36 nM min^{-1} for macroH2A nucleosomes. In the bottom panel, initial rates when 160 nM H2A or macroH2A nucleosomes are remodeled separately are 21.5 ± 0.85 nM min^{-1} for H2A nucleosomes and 14.5 ± 0.80 nM min^{-1} for macroH2A nucleosomes. The similar 1.5-fold rate difference between the two nucleosomes under competition and separate conditions shows that they compete equally for ACF binding. Rates are means and standard deviations from three independent trials.

buffer containing 0.5 M NaCl in 25 mM Hepes (pH 7.4), 0.1 mM EDTA, 0.5 mM EGTA, 0.02% Igepal CA-630 (v/v) (Sigma), 2 mM MgCl$_2$, 20% glycerol (v/v), 1 mM PMSF, 1 mM DTT, and protease inhibitors. Dimer was then eluted with 10 c.v. total of increasing NaCl concentrations (0.6, 0.7, 2 × 0.75, 2 × 0.8, 2 × 0.85, 0.9, and 1 M). Purified dimer was confirmed and quantified by SYPRO red staining (Invitrogen) on a 15% SDS−acrylamide gel.

Histones H2A, H2B, mH2A-HD, H3, and H4 were purified as previously described (*8, 14*). H2A/H2B dimer, mH2A-HD/H2B dimer, and H3/H4 tetramer were assembled by refolding individual histones together by dialysis out of unfolding buffer [7 M guanidinium, 20 mM Tris (pH 7.5), and 10 mM DTT] into refolding buffer containing 2 M NaCl, 10 mM Tris (pH 7.5), 1 mM EDTA, and 5 mM 2-mercaptoethanol. The tetramer and dimers were purified away from aggregates by size-exclusion chromatography on a Superdex

200 HR 10/30 column (GE Healthcare) (*14*). MacroH2A and macroH2A-HD nucleosomes were assembled by mixing a 3:1:1 molar ratio of macroH2A/H2B dimer, tetramer, and DNA followed by salt gradient dialysis as previously described (*9*). Properly assembled nucleosomes were subsequently isolated through glycerol gradient ultracentrifugation in the presence of 0.1% Igepal CA-630. Stoichiometric ratios of histones in the purified nucleosomes were confirmed through SYPRO red staining. Nucleosomes containing H2A were assembled as described above, at a 2:1:1 H2A/H2B dimer:tetramer:DNA molar ratio, or from octamer as previously described (*14*). Briefly, octamer was assembled by mixing H2A, H2B, H3, and H4 in a molar ratio of 1.2:1.2:1:1 in unfolding buffer and dialyzing into refolding buffer (*14*). Octamer was then purified by size exclusion before assembly onto equimolar quantities of DNA template through salt dialysis and subsequent glycerol gradient purification as described above. The two methods used for assembling H2A-containing nucleosomes did not alter the histone composition as determined by SYPRO red staining or the basic nucleosome properties as determined by mobility on native polyacrylamide gels.

Gel Mobility Shift Experiments. Human SWI/SNF gel mobility shift experiments were performed in reaction buffer containing 40 mM KCl, 3 mM MgCl$_2$, 0.04% Igepal CA-630, 12% glycerol, 0.64 mM EDTA, 8 mM HEPES (pH 8), and 8 mM Tris (pH 7.5). Saturating enzyme conditions included 30 nM hSWI/SNF mixed with 10 nM nucleosome and 2 mM ATP. For limiting enzyme conditions, including direct competition between H2A- and macroH2A-containing nucleosomes, 12 nM hSWI/SNF and 60 nM total nucleosomes were used. This substrate concentration was significantly higher than the published K_d values for SWI/SNF (*15*). Reaction mixtures were incubated at 30 °C and reactions stopped with a mix of ADP and competing stop plasmid DNA as previously described (*13*). Resulting products were run on native 5% (v/v) polyacrylamide gels run in 0.5× TBE and visualized by SYBR gold staining (Invitrogen) on a Typhoon Variable Mode Imager (Amersham). ImageQuant (GE Healthcare) was used to quantify band intensities, which were used to calculate the fraction of total nucleosomes corresponding to the unremodeled state for each time point, normalized to time zero. We note that, at time zero, in addition to the major nucleosomal bands marked in the figures, there are other minor species of histone−DNA complexes that migrate at different rates. These are most likely nucleosomes positioned differently on the DNA template or other histone−DNA complexes. However, the major starting nucleosome band is cleanly distinguishable from both the additional and product bands. We therefore assessed remodeling by quantifying how the major substrate band changed over time as a fraction of all the bands visible on the gel.

For the single-turnover experiments, rate constants were determined by fitting the fraction of nucleosomes repositioned over time to a single exponential. For the multiple-turnover experiments in Figures 2 and 3A, initial rates were obtained from the first 5 min of the reaction, which corresponds to the linear region of the time course. Data shown for the multiple-turnover experiments were fit by excluding the minor bands from the quantification. However,
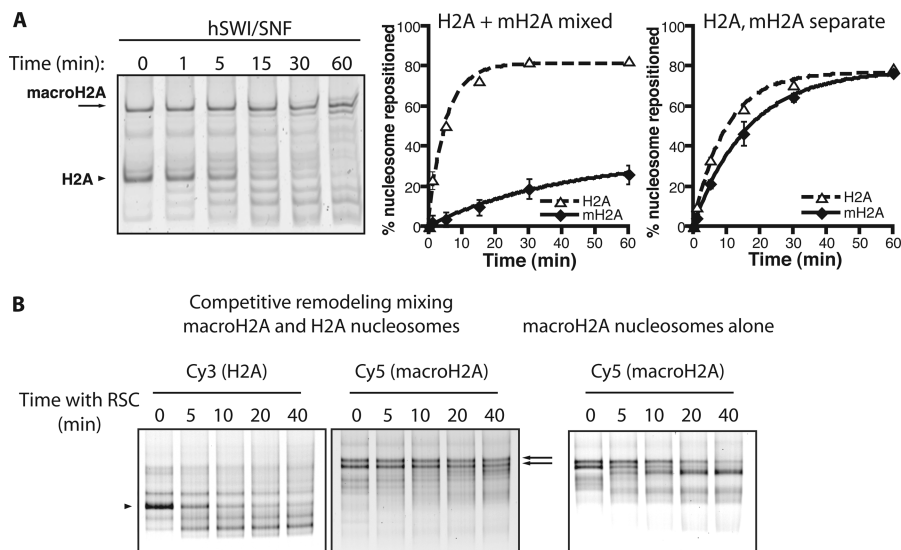
FIGURE 3: SWI/SNF family complexes are preferentially recruited to H2A nucleosomes. (A) In the left panel, 30 nM H2A and 30 nM macroH2A 20/60 nucleosomes were mixed together with 12 nM hSWI/SNF and visualized on the same gel. In the middle panel, initial remodeling rates from the left panel are 3.1 ± 0.54 nM min^{-1} for H2A nucleosomes and 0.23 ± 0.056 nM min^{-1} for macroH2A nucleosomes. In the right panel, when remodeled separately, initial rates are 4.1 ± 0.34 nM min^{-1} for H2A nucleosomes and 2.5 ± 0.016 nM min^{-1} for macroH2A nucleosomes. Values were calculated from two independent experiments. (B) In the left and middle panels, H2A nucleosomes assembled onto Cy3-labeled 54A18 DNA were mixed with an equal quantity of macroH2A nucleosomes assembled on Cy5-labeled DNA and visualized separately. After incubation for 40 min with RSC, 57% of H2A nucleosomes are removed from the original location while only 7% of macroH2A nucleosomes were repositioned in the same reaction (~18-fold difference). In the right panel, in comparison, when macroH2A nucleosomes were incubated alone with RSC, 52% of nucleosomes were repositioned from their original location after 40 min. Long arrows denote unremodeled macroH2A nucleosomes and short arrows unremodeled H2A nucleosomes.
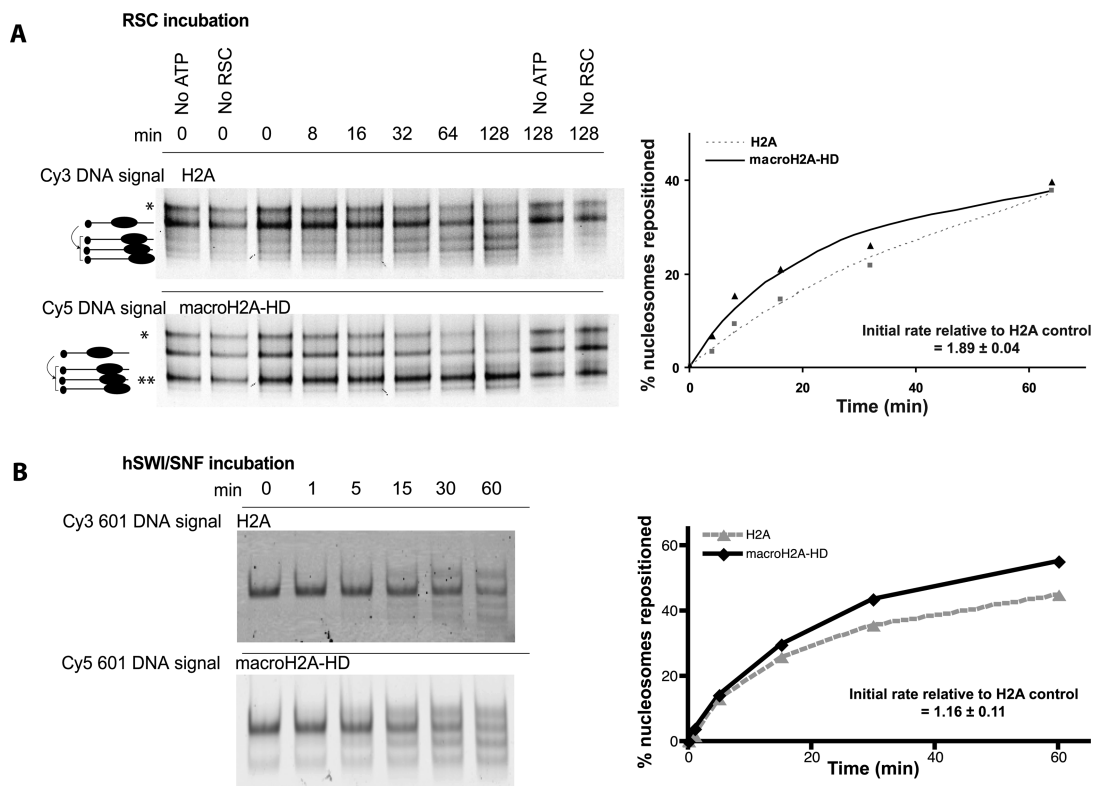

FIGURE 4: SWI/SNF complexes are recruited equally well to macroH2A histone fold (macroH2A-HD) nucleosomes and H2A nucleosomes. (A) RSC (40 nM) was used to reposition H2A and macroH2A-HD nucleosomes. The sum of all downshifted positions was measured relative to the initial +70 position (right panel). A proportion of nucleosomes is deposited at an additional position designated with an asterisk that has been described previously and not used in analysis (16). In addition, a substantial proportion of macroH2A-HD nucleosomes was deposited at the location designated with two asterisks. (B) H2A (30 nM) and macroH2A-HD (30 nM) nucleosomes were mixed together with 12 nM hSWI/SNF. The DNA of the macroH2A-HD nucleosomes is end-labeled with Cy5 and that of H2A nucleosomes with Cy3.

this did not alter the relative rates of remodeling for macroH2A versus H2A nucleosomes (data not shown).

Yeast SWI/SNF and RSC competition reactions were performed using each nucleosome sample at 0.1 mM in a

A

Altered SWI/SNF
conformation

B

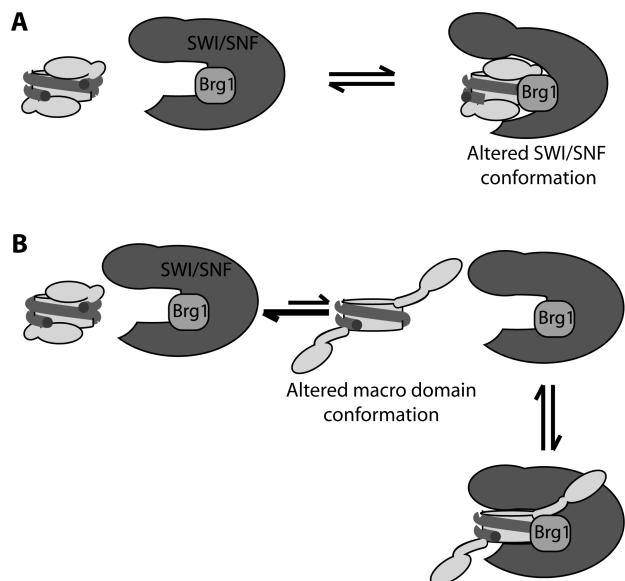Altered macro domain
conformation

FIGURE 5: Two models for the inhibition of SWI/SNF binding caused by the macro domain. (A) Steric hindrance due to the altered shape of a macroH2A nucleosome may require SWI/SNF complexes to change conformation to bind. (B) The linker region of macroH2A may adopt multiple conformations, only some of which allow binding of SWI/SNF to that nucleosome.

reaction buffer containing 50 mM NaCl, 50 mM Tris (pH 7.5), 3 mM MgCl₂, and 1 mM ATP. Samples were incubated at 30 °C with the amount of remodeling enzyme and for the times specified in the figures. The reactions were stopped by adding 500 ng of *Hin*dIII-digested bacteriophage lambda competitor DNA and 5% (w/v) sucrose and placing the mixtures on ice. Samples were run onto prepared $0.2\times$ Tris-borate-EDTA-5% native polyacrylamide gels for 3 h at 300 V at 4 °C with pump recirculation. The gels were scanned in a Fuji Phosphoimager FLA-5100 instrument, and the bands were quantitated with Aida (Fujifilm). End positions of nucleosomes are labeled in the figures as previously described (*16*). The initial rates were determined by measuring the intensity at the end position(s) relative to the sum of the initial and end positions. The data were adjusted to give 0% repositioned at time zero. The values were fitted nonlinearly to a hyperbolic curve using the Solver add-in function in Microsoft Excel over 1000 iterative cycles. The initial rate was calculated by differentiation of the curve, to extrapolate the linear part of the reaction and solve for the point at which time equals zero. For each comparison, the rate of macroH2A−HD nucleosomes was divided by that of major-type H2A to determine the relative rate. The initial rate, mean and standard deviation, was determined from triplicate measurements.

ACF gel mobility shift experiments were performed at 30 °C in ACF reaction buffer [30 mM KCl, 3 mM MgCl₂, 0.05% Igepal CA-630, 12% glycerol, 0.56 mM EDTA, 6 mM HEPES (pH 8), and 10 mM Tris (pH 7.5)]. Because hACF activity under saturating ATP conditions is on a time scale too fast to be accurately measured by gel shift analysis, we used a subsaturating ATP concentration of 4 μM. For saturating enzyme conditions, 25 nM hACF was mixed with 10 nM nucleosomes and incubated for the times indicated. For limiting enzyme conditions, 5 nM hACF and a saturating concentration of 160 nM total nucleosome were used based on previous work and data not shown (*17*). The reactions

were processed and the data quantified as described for the human SWI/SNF experiments.

RESULTS

A key step in salt dialysis-mediated assembly of nucleosomes is the dissociation of the H2A/H2B dimer from the H3/H4 tetramer before association with DNA. However, a recent study has shown that preassembled octamers containing macroH2A remain stable from 2 to 0.5 M NaCl. Because deposition of the tetramer onto DNA during in vitro nucleosome assembly occurs at ∼1 M NaCl, the unusual stability of mH2A octamers is thought to inhibit this key step and result in nucleosomes with noncanonical structures (*9*). We therefore independently reinvestigated the activity of SWI/SNF and ACF complexes on macroH2A nucleosomes assembled from individually purified macroH2A/H2B dimers and H3/H4 tetramers to ensure proper ordered deposition of the histones (Experimental Procedures). Proper histone content was confirmed using SYPRO red staining (Figure 1 of the Supporting Information).

To re-examine the effects of macroH2A on ATP-dependent chromatin remodeling, we dissected its effects on both the maximal rate of chromatin remodeling and binding by the complexes. To determine the effects on the maximal rate of remodeling, we used excess and saturating remodeling complex and measured remodeling activity by the native gel shift. As previously shown, SWI/SNF forms a variety of products, most of which migrate faster than the unremodeled 20/60 nucleosomes. In contrast, hACF products migrate slower than its 0/80 nucleosomal substrate (Figure 1A). In each case, saturating conditions were confirmed by showing that the maximal rates were the same across a 2−5-fold variation in enzyme concentration (*13, 15*). Under these single-turnover conditions, hSWI/SNF and ACF both remodel the two types of nucleosomes at similar maximal rates (Figure 1B,C; complete gels available in Figure 2 of the Supporting Information).

These results suggest macroH2A nucleosomes are excellent substrates for remodeling by hSWI/SNF and hACF. However, because these experiments were carried out with saturating enzyme, they cannot reveal any differences in binding. Previous work has shown that SWI/SNF and ACF complexes bind to nucleosomes with K_d values in the lower nanomolar range, making it technically challenging to measure absolute binding affinities, because it is difficult to avoid titration conditions (*18*). We therefore measured relative binding affinities by setting up a competition between macroH2A and H2A nucleosomes. Such an assay has been previously used to determine which of two chromatin substrates is the preferred binding partner of SWI/SNF (*19*). Our competitive reactions were designed such that a limiting amount of remodeling complex would have to choose between excess and equal concentrations of each type of nucleosome. Under these conditions, the enzyme partitions between the two types of nucleosomes in proportion to its K_d for each nucleosome and, once bound, remodels each type of nucleosome with its respective maximal rate. As a result, the relative rates of remodeling reflect differences in binding affinity as well as differences in maximal rates of remodeling. Our results (Figure 1B) indicate that both types of nucleosomes are remodeled at similar maximal rates by SWI/SNF.

ACF also remodeled both types of nucleosomes at similar maximal rates under the conditions specified (Figure 1C). Therefore, in our competitive remodeling assays, the relative rates of remodeling essentially reflect differences in binding affinity.

hACF remodels both types of nucleosomes with similar rates when they are presented to hACF individually (Figure 2, bottom panel, and Figure 3 of the Supporting Information). When the two types of nucleosomes are mixed, ACF still remodels them with similar rates (Figure 2, top and middle panels). This indicates that hACF does not have a strong preference for binding either type of nucleosome. If hSWI/SNF is presented with each nucleosome separately, both types of nucleosomes are remodeled with similar rates (Figure 3A, right panel). If, however, the two types of nucleosomes are mixed and competing for the same hSWI/SNF molecules, H2A-containing nucleosomes are remodeled much more rapidly than macroH2A-containing nucleosomes (Figure 3A, left and middle panels). When normalized to the slightly different rates of nucleosome remodeling observed for each nucleosome alone, hSWI/SNF prefers H2A over macroH2A nucleosomes by 9-fold.

Interestingly, the RSC complex, a major yeast member of the SWI/SNF family, also prefers to bind H2A nucleosomes over macroH2A-containing nucleosomes. In these experiments, nucleosomes were assembled onto a fragment of DNA derived from the MMTV promoter (Figure 1A). When presented with macroH2A nucleosomes alone, RSC is able to efficiently remodel the nucleosomes (Figure 3B, right panel). However, like hSWI/SNF, RSC preferentially remodels H2A nucleosomes over macroH2A nucleosomes under competitive conditions (Figure 3B, left and center panels).

We next re-examined if, as previously proposed, nucleosomes containing just the histone domain of macroH2A are poor substrates for SWI/SNF. We find that RSC (Figure 4A) and hSWI/SNF (Figure 4B) do not show a strong preference for H2A nucleosomes in competition with nucleosomes containing just the histone domain of macroH2A. This indicates that the reduced level of recruitment of SWI/SNF complexes to macroH2A nucleosomes seen in Figure 3 is due to the macro domain.

DISCUSSION

Our results indicate that, in contrast to previous results, macroH2A nucleosomes can be efficiently remodeled by both SWI/SNF and ACF complexes. Interestingly, while we find macroH2A does not affect the maximal rates of remodeling, it specifically reduces the level of recruitment of SWI/SNF but not ACF. Further, in contrast to the previous observations that nucleosomes with only the histone domain of macroH2A are poor substrates for SWI/SNF, we find that the histone domain of macroH2A behaves almost identically to H2A in all our assays.

The observation that yeast RSC also preferentially interacts with H2A nucleosomes suggests that the mammal-specific macroH2A may function in part by utilizing conserved differences between ACF and SWI/SNF remodelers. SWI/SNF complexes are large and contain at least eight different subunits (20−23). ACF is significantly smaller and consists

of only two subunits (24). Binding to macroH2A nucleosomes may require some structural rearrangement in the larger SWI/SNF complexes to accommodate the sizable macro domains (Figure 5A). It is also possible that the most stable arrangement of the macro domain blocks productive SWI/SNF binding and that the macro domain must first be repositioned via the flexible linker region to allow SWI/SNF binding and subsequent activity (Figure 5B).

Our results suggest one strategy by which macroH2A can help maintain gene silencing. While SWI/SNF family complexes are more often involved in gene activation (25, 26), ACF is primarily involved in gene silencing (27, 28). This is linked to ACF's ability to position nucleosomes equidistant from each other, an apparent prerequisite for heterochromatin establishment (24, 28). ACF is also associated with Polycomb group proteins, of which Polycomb complex PRC1 was recently found to be required in the early maintenance of the inactive X chromosome (3). Thus, to selectively maintain heterochromatin and prevent transcription, macroH2A may have evolved to preferentially allow binding by the repressive ACF complexes over the activating SWI/SNF complexes. In a model where different ATP-dependent remodeling complexes compete to fulfill their functions, one role of macroH2A may be to shift the balance in favor of maintenance of repressive chromatin, while still maintaining the ability to be remodeled by activating remodeling complexes should they be recruited at sufficient levels.

SUPPORTING INFORMATION AVAILABLE

Quantification of the proper stoichiometry of assembled macroH2A nucleosomes and full gels from each gel shift remodeling assay. This material is available free of charge via the Internet at http://pubs.acs.org.

REFERENCES

1. Pehrson, J. R., and Fried, V. A. (1992) MacroH2A, a core histone containing a large nonhistone region. *Science 257*, 1398–1400.
2. Costanzi, C., and Pehrson, J. R. (1998) Histone macroH2A1 is concentrated in the inactive X chromosome of female mammals. *Nature 393*, 599–601.
3. Hernandez-Munoz, I., Lund, A. H., van der Stoop, P., Boutsma, E., Muijrers, I., Verhoeven, E., Nusinow, D. A., Panning, B., Marahrens, Y., and van Lohuizen, M. (2005) Stable X chromosome inactivation involves the PRC1 Polycomb complex and requires histone MACROH2A1 and the CULLIN3/SPOP ubiquitin E3 ligase. *Proc. Natl. Acad. Sci. U.S.A. 102*, 7635–7640.
4. Agelopoulos, M., and Thanos, D. (2006) Epigenetic determination of a cell-specific gene expression program by ATF-2 and the histone variant macroH2A. *EMBO J. 25*, 4843–4853.
5. Zhang, R., Poustovoitov, M. V., Ye, X., Santos, H. A., Chen, W., Daganzo, S. M., Erzberger, J. P., Serebriiskii, I. G., Canutescu, A. A., Dunbrack, R. L., Pehrson, J. R., Berger, J. M., Kaufman, P. D., and Adams, P. D. (2005) Formation of MacroH2A-containing senescence-associated heterochromatin foci and senescence driven by ASF1a and HIRA. *Dev. Cell 8*, 19–30.
6. Doyen, C. M., An, W., Angelov, D., Bondarenko, V., Mietton, F., Studitsky, V. M., Hamiche, A., Roeder, R. G., Bouvet, P., and Dimitrov, S. (2006) Mechanism of polymerase II transcription repression by the histone variant macroH2A. *Mol. Cell. Biol. 26*, 1156–1164.

7. Angelov, D., Molla, A., Perche, P. Y., Hans, F., Cote, J., Khochbin, S., Bouvet, P., and Dimitrov, S. (2003) The histone variant macroH2A interferes with transcription factor binding and SWI/SNF nucleosome remodeling. *Mol. Cell 11*, 1033–1041.

8. Chakravarthy, S., Gundimella, S. K., Caron, C., Perche, P. Y., Pehrson, J. R., Khochbin, S., and Luger, K. (2005) Structural characterization of the histone variant macroH2A. *Mol. Cell. Biol. 25*, 7616–7624.

9. Chakravarthy, S., and Luger, K. (2006) The histone variant macro-H2A preferentially forms "hybrid nucleosomes". *J. Biol. Chem. 281*, 25522–25531.

10. Sif, S., Stukenberg, P. T., Kirschner, M. W., and Kingston, R. E. (1998) Mitotic inactivation of a human SWI/SNF chromatin remodeling complex. *Genes Dev. 12*, 2842–2851.

11. Ferreira, H., Flaus, A., and Owen-Hughes, T. (2007) Histone modifications influence the action of Snf2 family remodelling enzymes by different mechanisms. *J. Mol. Biol. 374*, 563–579.

12. Aalfs, J. D., Narlikar, G. J., and Kingston, R. E. (2001) Functional differences between the human ATP-dependent nucleosome remodeling proteins BRG1 and SNF2H. *J. Biol. Chem. 276*, 34270–34278.

13. Yang, J. G., Madrid, T. S., Sevastopoulos, E., and Narlikar, G. J. (2006) The chromatin-remodeling enzyme ACF is an ATP-dependent DNA length sensor that regulates nucleosome spacing. *Nat. Struct. Mol. Biol. 13*, 1078–1083.

14. Luger, K., Rechsteiner, T. J., and Richmond, T. J. (1999) Preparation of nucleosome core particle from recombinant histones. *Methods Enzymol. 304*, 3–19.

15. Narlikar, G. J., Phelan, M. L., and Kingston, R. E. (2001) Generation and interconversion of multiple distinct nucleosomal states as a mechanism for catalyzing chromatin fluidity. *Mol. Cell 8*, 1219–1230.

16. Flaus, A., and Owen-Hughes, T. (2003) Dynamic properties of nucleosomes during thermal and ATP-driven mobilization. *Mol. Cell. Biol. 23*, 7767–7779.

17. He, X., Fan, H. Y., Narlikar, G. J., and Kingston, R. E. (2006) Human ACF1 alters the remodeling strategy of SNF2h. *J. Biol. Chem. 281*, 28636–28647.

18. Fersht, A. (1999) *Structure and Mechanism in Protein Science*, W. H. Freeman and Co., New York.

19. Yudkovsky, N., Logie, C., Hahn, S., and Peterson, C. L. (1999) Recruitment of the SWI/SNF chromatin remodeling complex by transcriptional activators. *Genes Dev. 13*, 2369–2374.

20. Leschziner, A. E., Saha, A., Wittmeyer, J., Zhang, Y., Bustamante, C., Cairns, B. R., and Nogales, E. (2007) Conformational flexibility in the chromatin remodeler RSC observed by electron microscopy and the orthogonal tilt reconstruction method. *Proc. Natl. Acad. Sci. U.S.A. 104*, 4913–4918.

21. Leschziner, A. E., Lemon, B., Tjian, R., and Nogales, E. (2005) Structural studies of the human PBAF chromatin-remodeling complex. *Structure 13*, 267–275.

22. Asturias, F. J., Chung, W. H., Kornberg, R. D., and Lorch, Y. (2002) Structural analysis of the RSC chromatin-remodeling complex. *Proc. Natl. Acad. Sci. U.S.A. 99*, 13477–13480.

23. Skiniotis, G., Moazed, D., and Walz, T. (2007) Acetylated histone tail peptides induce structural rearrangements in the RSC chromatin remodeling complex. *J. Biol. Chem. 282*, 20804–20808.

24. Ito, T., Levenstein, M. E., Fyodorov, D. V., Kutach, A. K., Kobayashi, R., and Kadonaga, J. T. (1999) ACF consists of two subunits, Acf1 and ISWI, that function cooperatively in the ATP-dependent catalysis of chromatin assembly. *Genes Dev. 13*, 1529–1539.

25. Fan, H. Y., Narlikar, G. J., and Kingston, R. E. (2004) Noncovalent modification of chromatin: Different remodeled products with different ATPase domains. *Cold Spring Harbor Symp. Quant. Biol. 69*, 183–192.

26. Sudarsanam, P., and Winston, F. (2000) The Swi/Snf family nucleosome-remodeling complexes and transcriptional control. *Trends Genet. 16*, 345–351.

27. Deuring, R., Fanti, L., Armstrong, J. A., Sarte, M., Papoulas, O., Prestel, M., Daubresse, G., Verardo, M., Moseley, S. L., Berloco, M., Tsukiyama, T., Wu, C., Pimpinelli, S., and Tamkun, J. W. (2000) The ISWI chromatin-remodeling protein is required for gene expression and the maintenance of higher order chromatin structure in vivo. *Mol. Cell 5*, 355–365.

28. Fyodorov, D. V., Blower, M. D., Karpen, G. H., and Kadonaga, J. T. (2004) Acf1 confers unique activities to ACF/CHRAC and promotes the formation rather than disruption of chromatin in vivo. *Genes Dev. 18*, 170–183.